In-plane anisotropic photoresponse in all-polymer planar microcavities

Robert J. Knarr III,[a,†] Giovanni Manfredi,[a] Elisa Martinelli,[b] Matteo Pannocchia,[b] Diego Repetto,[c] Carlo Mennucci,[c] Ilaria Solano,[c] Maurizio Canepa,[c] Francesco Buatier de Mongeot,[c] Giancarlo Galli,[b] Davide Comoretto[a]

a) Dipartimento di Chimica e Chimica Industriale, Università degli Studi di Genova, via Dodecaneso 31, 16146 Genova (Italy).

b) Dipartimento di Chimica e Chimica Industriale, Università degli Studi di Pisa, via Moruzzi 13, 56124 Pisa (Italy).

c) Dipartimento di Fisica, Università degli Studi di Genova, via Dodecaneso 33, 16146 Genova (Italy).

† Present Address: Department of Chemistry, University of Basel, St. Johanns-Ring 19, 4056-Basel (CH).

Supplementary Information available: Absorption and cavity mode spectra after different cycles of writing/erasing process; AFM and interference microscopy data of PMA4 films; All-optical photomodulation at the third order PBG; effects of thermal photomodulation.

ABSTRACT

We report on the optical photomodulation properties of all-polymer planar microcavities in which the photochromic poly((4-pentyloxy-3'-methyl-4'-(6-methacryloxyhexyloxy))azobenzene) (PMA4) acts as photoresponsive cavity layer. We induce the trans-cis isomerization process of the azobenzene group by polarized 405 nm CW-laser irradiation, while the backward process is driven by unpolarized CW-laser irradiation at 442 nm. The all-optical photoisomerization process induces a remarkable in-plane anisotropic spectral shift of the cavity modes for the first and second order photonic band gaps. The spectral and intensity modulation effects for these flexible all-polymer microcavities are discussed with respect to those so far reported in literature for analogous systems.

Keyword: photochromic polymers, photonic crystals, microcavity

Introduction

Polymers containing azobenzene pendant groups are suitable materials for many applications including photo-actuators,[1-2] molecular motors,[3] photoswitching systems,[4] conductance switches,[5-6] and optical memories.[7] The *trans-cis* isomerization (and vice-versa) may occur following irradiation with UV-visible light, mechanical stress, or electrostatic stimulation.[8] Trans-to-cis photoisomerization of the azo group occurs rapidly while the lifetime of the thermodynamically less stable *cis* form can be very long depending on the chemically tailored polymer structure.[9-10]
It is interesting to remind that the azobenzene groups in their *trans* form are mesogenic and favor formation of a liquid crystal mesophase, typically nematic, whereas they are disorderly arranged in an isotropic phase when in their *cis* form.[10-11] Moreover, the photoisomerization process is accompanied by a rearrangement in the spatial configuration of the compound,[12-13] and when polarized light is used, alignment of azobenzene moieties induces anisotropies that modify the optical response of the material.[10-11,13] The absorption spectra of azo-derivatives show mainly two peaks assigned to the $\pi \rightarrow \pi^*$ transition (about 350 nm) and to the symmetry forbidden $n \rightarrow \pi^*$ transition (about 450 nm). The $\pi \rightarrow \pi^*$ transition is more intense for the *trans* azobenzene while the $n \rightarrow \pi^*$ peak possesses a higher oscillator strength for the *cis* form.[10] The absorption of photons with such energies allows reversible photo-isomerization, even though the quantum efficiencies of the back and forth processes are not equal.[4,8-9,14-15]
From the photonic point of view, the photoisomerization process is appealing since inducing a modification of the real part of the refractive index (Δn), which can be used for different devices.[16-25] Novel opportunities are provided by exploiting such Δn to tune the optical response of photonic crystals (PhC), i.e. periodical arrays of materials possessing different refractive index on a sub-micrometer scale. In PhC the coherent diffraction of light by the dielectric lattice planes generates a photonic band gap (PBG), i.e. a spectral region where photons cannot propagate into the structure thus being backward diffracted giving rise to a strong chromatic response. The spectral fingerprint of the PBG is a peak (minimum) in the reflectance (transmittance) spectrum of the PhC. The spectral position of the PBG is dictated only by the periodicity of the dielectric lattice and by the difference in the refractive index of the composing materials (dielectric contrast).[26-27] When one of them is a photochromic material, the Δn associated with the photoisomerization process is expected to modify the PBG properties since affecting the dielectric contrast. In this way, innovative all-optical switching, modulation or limiting devices can be envisaged,[28] In this respect, the PhC behaves as a transducer of the photoisomerization process (detected in the absorption spectra at the blue-UV wavelengths) into a "chromatic" effect occurring in any desired spectral range of interest (for instance in the near infrared at telecommunication windows). Even though different organic and hybrid photonic crystal structures have been already tested in the field [29-37], recently the use of all-polymer planar structures like multilayers (i.e. Distributed Bragg Reflectors, DBR) or planar microcavities (i.e. multilayers where the periodicity along one direction is broken by a structural defect) gained an increasing interest.[27] Indeed, such structures have been shown to be efficient for vapor sensing,[38] fluorescence enhancement[39-40] and lasing.[41-44] When photochromic azo-polymers are embedded into DBRs, very strong and efficient intensity photomodulation of the reflectance spectrum has been demonstrated making the system interesting for display applications as demonstrated by the Kurihara' group.[45-46] Additional opportunities are provided by using more refined structures such as the planar microcavity since the engineered periodicity defect there inserted generates an allowed state (the cavity mode) within the forbidden PBG. Due to the stronger spatial localization of light provided by microcavities with respect to DBR, light-matter interaction is there deeply modified.[27]
For this reason, we have prepared all-polymer microcavities where the defect layer is made by poly((4-pentyloxy-3'-methyl-4'-(6-methacryloxyhexyloxy))azobenzene) (PMA4, Figure 1a), a photochromic polymer carrying one azobenzene pendant groups for each monomer unit. CW polarized/unpolarized photomodulation of the microcavities gives rise to large and in-plane anisotropic spectral shifts as well as to intensity modulation of cavity modes. The photomodulation is also observed for multiple diffraction PBG orders at different spectral ranges.

Experimental

PMA4 was synthesized according to a literature procedure.[23] Weight and number average molar masses (M_w = 181500 g mol^{-1} and M_n = 47500 g mol^{-1}) were determined by size exclusion chromatography. Glass transition and nematic-isotropic (NI) transition temperatures, T_g = 35 °C and T_{NI} = 85 °C, were measured by differential scanning calorimetry. PMA4 films were prepared by spin-coating its toluene (Sigma-Aldrich, 99.8%) solutions with concentrations of 30 or 60 mg mL^{-1} at a spinning rate in the range 10-100 rps. Films are quite uniform on an area of about 24x24 mm^2 and have thicknesses varying from tens of nanometers to about one micrometer. PMA4 solutions at the higher concentrations are very viscous, thus reducing film uniformity at the lowest spinning velocities.
The microcavities are composed of two Distributed Bragg Reflectors (DBRs) that encapsulate the engineered defect. The two DBRs are prepared by spin coating, a reliable technique already tested for the preparation of multilayered structures [39,44,47-49]: they are made by 15 alternating layers of poly(N-vinylcarbazole) (PVK) and Cellulose Acetate (CA) (concentration, about 30 mg mL^{-1}; spin velocity, 55 rps, thickness d_{CA}=272 nm, d_{PVK}= 156 nm, d_{PVA}= 100 nm). PVK was supplied by Acros Organics and is used as high refractive index material (n~1.69), while CA is supplied by Sigma-Aldrich and is used as low refractive index material (n~1.46). Since toluene (the solvent for PMA4) and diacetone alcohol (the solvent for CA) are not perfectly orthogonal solvents in our conditions, PMA4 cavity is sandwiched between two polyvinyl alcohol (PVA) layers. The PVA (supplied by Sigma-Aldrich) is dissolved in a mixture of equal parts of water and ethanol. This mixture dissolves neither CA nor PVK and is immiscible with toluene. In this way, the defect surrounded by the two DBRs is composed

not of a single layer but of three layers: the external PVA ones and the internal one made by PMA4 (about 928 nm thick, see Fig. SI3 in Supplementary Information). The structure of the entire system is sketched in Figure 1b. The microcavity can be peeled-off from the substrate where is grown and then bent or folded.

The back and forth photochromic transition is driven by a polarized continuous-wave (CW) laser at 405 nm Oxxius SN LAS-00676, 50 mW sample spot ~4 mm diameter ("writing" laser) and by an unpolarized 40 mW CW laser at 442 nm CNI MDL-III-442, sample spot 3 mm diameter ("erasing" laser). In order to prevent possible thermal induced effects, particular care was used to limit the exposure time of the cavity to the writing/erasing beam. According to the data reported in Fig. SI1c, we notice that the writing process is very fast, while the erasing one presents a long time (several minutes) tail. Then, the writing process usually lasts for a few seconds (depending also on the laser power and PMA4 film thickness), while the erasing one lasts for about a couple of minutes.

The optical spectra (transmittance and near-normal incidence reflectance spectra) were collected using setups based on optical fiber coupled with an Avantes 2048 XL spectrometer (200–1100 nm, resolution 1.4 nm), an Ocean Optics Jazz compact modular spectrometer (350-550 nm and 530-880 nm, 0.5 nm resolution) or with an Arcoptics FT-interferometer (900-2600 nm, resolution 8 cm^{-1}). For the photomodulation measurements the highest resolution spectrometer was used. The light source was a combined deuterium–halogen lamp Micropak DH2000BAL. A Glan-Taylor polarizer was used to polarize light either parallel (LP, like polarized) or perpendicular (ULP, un-like polarized) to the one of the writing laser.

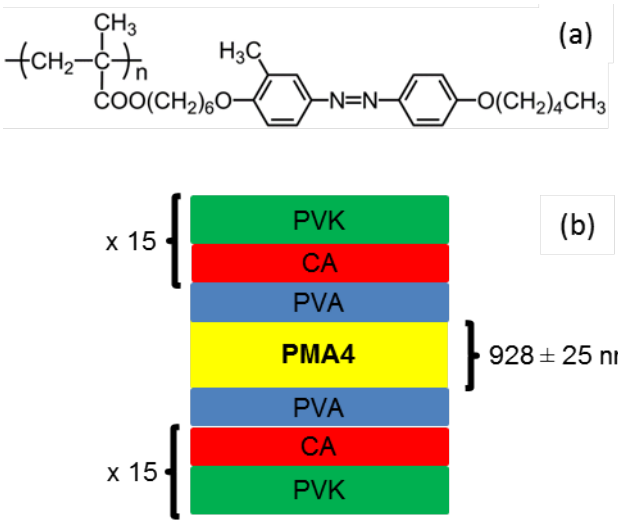

Fig. 1. a) Chemical structure of PMA4. b) Sketch of the microcavity's structure.

The morphological characterization of PMA4 thin films was performed by a commercial Nanosurf Atomic Force Microscope (AFM). Surface polymer images have been acquired in three different states: on the as-spun film, after writing and after erasing. The thickness of PMA4 film was measured by AFM in the three different states. The film was mechanically scratched to remove the polymer from the underlying fused silica substrate (see for instance Figure SI3a). Afterwards, AFM images were acquired along the step. The step height thus corresponds to the film thickness. During routine multilayered structures preparation, film thicknesses have been measured by light interferometry using a GBS smart WLI microscope with a 20× interference objective. We found a reasonable agreement between AFM and interference microscopy thickness measurements, although it seems that the latter slightly overestimate the film thickness.

Each image has been processed with WSxM software[50] by means of the following procedure: first, an offset flatten has been performed in order to remove low frequency noise (this noise can be seen as an irregular distribution of the scan height along the Y direction). Offset flatten works by subtracting a constant function (the average of each line) to each scan in the unprocessed image. Then, local plane operation has been made in order to force all points of the fused silica substrate at the same level (it corresponds to the reasonable assumption of a flat substrate on the image scale). Finally, the height histograms have been extracted from each image and plotted on the same graph (Fig, SI2 in Supplementary Information). Two peaks are clearly visible, one for the substrate (centered around zero nm) and one for the film (centered around 200 nm) with widths of the order of 1.5 nm. The distance between the two peaks represents the film thickness.

The absolute accuracy of the AFM microscope, verified on a microfabricated silicon calibration standard, was found to be in the range of 0.5 nm. From instrument data sheet, the nominal z measurement level noise is below 0.3 nm. The precision of the thickness measurement is thus dominated by the flatten procedure described above, i.e. by the width of the Gaussian peak centered around 0 nm. The HWHM values have been thus taken as error bars of the film thickness for each state: 1.0 nm for the as-spun, 1.3 nm after laser illumination at 405, and 1.5 nm after illumination at 442 nm.

Results and discussion

Figure 2a shows the absorbance spectra for thin PMA4 films as-spun, after irradiation with the writing laser (405 nm, linearly polarized) and after further irradiation with the erasing laser (442 nm, unpolarized). For the as-spun films, a strong absorption weakly structured is observed at 366 nm, followed by another structure at 250 nm. In addition, a tiny absorption tail is observed around 460 nm. After irradiation with the writing laser, the transition at 366 nm remarkably reduces in intensity and a structure around 320 nm appears while the peak at 250 nm is almost unchanged. Moreover, the shoulder at 460 nm gains intensity. When the film is then irradiated with the erasing beam, a reversed behavior is observed with an increase in the oscillator strength for the transition at 366 nm and a reduction of absorptions around 320 and 460 nm. Minor changes are observed for the 250 nm transition. Repeated writing (405 nm)/erasing (442 nm) cycles provide highly reproducible and reversible spectra as reported for different wavelengths in Figure SI1a of Supplementary Information. The mechanism underlying this change is explained in terms of the photochromic transition occurring in the azobenzene moieties. The $\pi \rightarrow \pi^*$ transition at about 360 nm is more intense for the azobenzene in *trans* form, while the

n→π* transition at about 460 nm possesses a higher oscillator strength in the *cis* form.[10,24,51] Even though our writing photons were not fully resonant with the main electronic transitions involved, the effects of photoisomerization can be clearly observed in the spectra. Moreover, the initial spectrum cannot be fully recovered by illumination with the erasing beam. In fact the photoinduced isomerization occurs between two states having different relative populations of *trans* and *cis* isomers. A sketch of the in-plane isomer population in the film during the photoisomerization process is reported in Figure 2b. After film preparation, all azobenzene moieties are randomly oriented in the thermodynamically stable *trans* form. After irradiation with the writing laser, absorbing molecules are turned to the *cis* form and their transition dipole moments partially rotate. Thus, the population of the *cis* isomer increases at the expenses of the population of *trans* isomer. The erasing laser radiation is mainly absorbed by the *cis* molecules regardless of their orientation thus isomerizing them back to the *trans* form without directional preference and reducing the population of *cis* one. We do not know the relative populations of *cis* and *trans* isomers at the photo-stationary state since the respective absorption coefficients cannot be evaluated. Only after heating for several hours an almost complete recovery to the as-spun state was achieved.

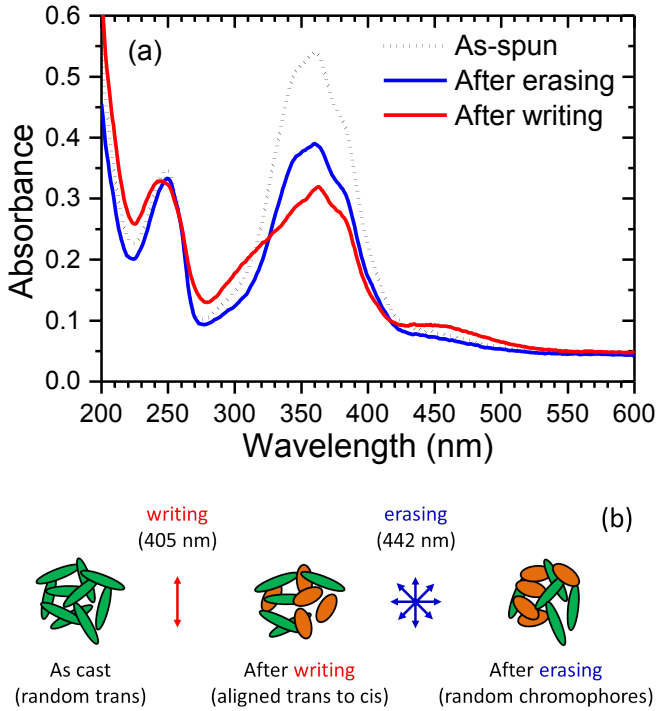

Fig. 2. a) Absorption spectra of PMA4 as-spun films (black dotted line), after exposure to writing laser (red solid line) and after exposure to the erasing beam (blue, solid line). b) Sketch of the mechanism underlying absorption modifications on irradiation

It is known that light beams might induce a structuring in azobenzene films, thus locally modifying their thickness and topography.[52] Since such surface structures could be detrimental to the properties of PhCs,[27] an Atomic Force Microscopy (AFM) morphological characterization of the PMA4 thin film was performed. Surface polymer images have been acquired in three different states: the as-spun film (Figure 3a), after writing (Figure 3b) and after erasing (Figure 3c). A clear change in morphology upon isomerization is observed.

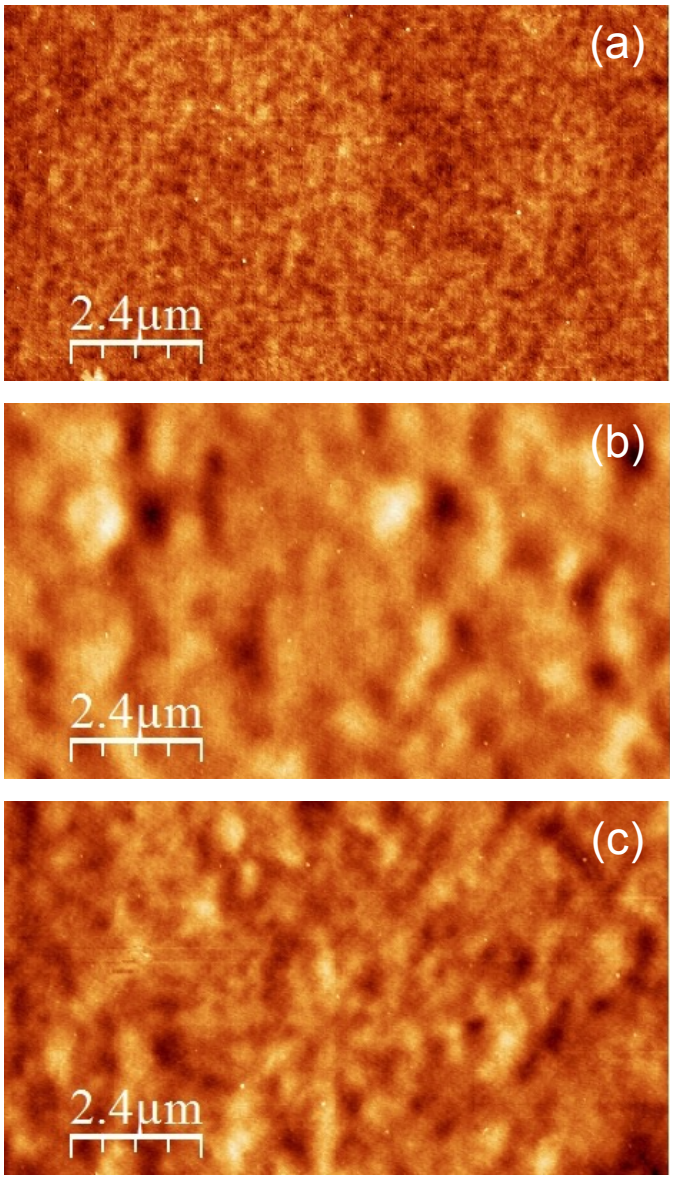

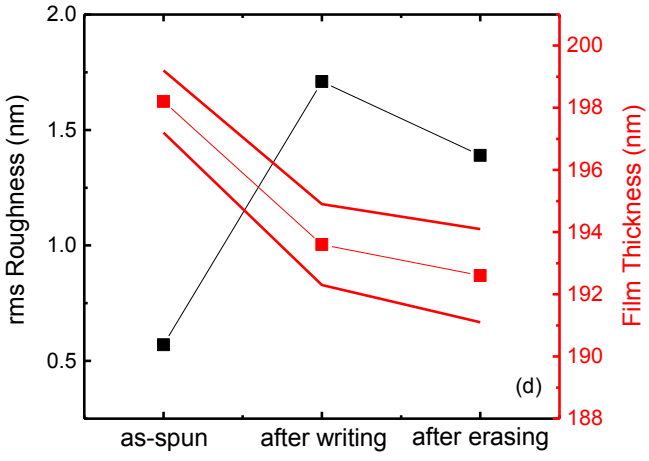

Fig. 3. AFM images on PMA4 films: a) as-spun, z scale 0-6 nm; b) after 1 minute laser illumination at 405 nm, z scale 0-15 nm; c) after 5 minutes laser illumination at 442 nm, z scale 0-15 nm. (d) Rms roughness and film thickness of PMA4 thin film in the three states.

After writing (Figure 3b), the polymer surface exhibits an increased root mean square (rms) roughness (1,7 nm) with respect to the as-spun surface film (rms roughness 0,6 nm, Figure 3a). The original morphology cannot be fully recovered by erasing, as shown in Figure 3c, with the film still presenting an increased rms roughness (1.4 nm) compared to the as-spun state.

The irradiation effect is well visible in the plot of the one-dimensional power spectral density (1D-PSD) (Figure 4) as a function of the spatial wavevector q=1/ξ, where ξ is the corrugation wavelength. The PSD is the Power Spectrum of the one-dimensional Fast Fourier Transform (1D-FFT) averaged over all rows in the slow scanning direction. Thus, PSD provides information on the presence of morphological corrugations with a specific wavevector "q=1/ξ". Data in Figure 4 shows the amplification of each harmonic component after writing (red curve), which results particularly evident at small q (with respect to the as-spun film, black curve). The effect is irreversible, as demonstrated by the 1D-PSD calculated on the film irradiated at 442 nm (blue curve). Since the area subtended the curves is proportional to the square of the rms roughness, it appears that the increased rms roughness upon isomerization is due to enhanced vertical corrugations modulated on larger spatial domain than 500 nm (wavevectors smaller than $2x10^6$ m^{-1}). Remarkably, on the small lateral scale below 500 nm (wavevectors larger than $2x10^6$ m^{-1}) no modifications of the local roughness are observed (i.e. black, red and blue lines are superimposed). We anticipate here that such roughness minimally affects the optical response of our microcavities (vide infra).

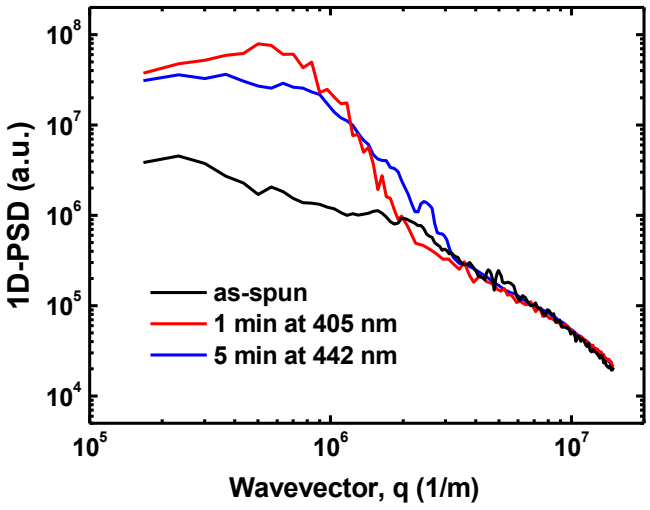

Fig. 4. One-dimensional power spectral density (1D-PSD) as a function of the spatial wavevector q=1/ξ.

AFM analysis was also used to accurately measure film thickness on scratched films (see Experimental section as well as Figure SI2 and Figure SI3 in Supplementary Information), which is essential (joint to the refractive indices) for engineering the PhC structure. The main drawback of AFM is the difficulty to use it during routinely multilayer film growth. However, its precision has been used to calibrate interference microscopy measurements, which instead can be performed during the growth (see Experimental section for details).

A change between the as-spun state and the illuminated one also occurs in the film thickness as measured by AFM. The as-spun thin film has a thickness of 198,0 ± 1,0 nm, while after writing the film has a smaller thickness of 193,0 ± 1,3 nm. After erasing, negligible film thickness changes are observed. It should be mentioned that such decrease refers to an average film height, which determines the position of the peak around 200 nm in the histogram of the heights (Figure 3d, as derived from Figure SI2 of Supporting Information). The higher surface roughness observed after writing, instead, determines an increase in the peak width.[53]

The observed effects in PMA4 thin film roughness and thickness upon irradiation have to be considered when the photomodulation properties of a complex structure such as a microcavity are investigated.

As has been previously demonstrated,[39-40,44,54] the spin coating technique allows to tune the spectral response of DBR and microcavities in any desired spectral range by changing the thickness of the CA or PVK layers forming the photonic structure. Moreover, their optical quality allows to observe in the optical spectra not only the first diffraction order, but also higher orders at shorter wavelengths. For these reasons, we decided to focus our investigation on microcavities having a photonic band gap in the Near Infrared (NIR) and higher orders in the visible to simultaneously probe the effect of the photochromic transition in different spectral regions of possible technological interest. Figure 5 shows the reflectance spectrum of a microcavity possessing the first order PBG at about 1300-1400 nm. The spectrum is dominated by three peaks at about 1370, 680 and 460 nm assigned to the first, second and third order PBGs, respectively. Within each peak, a sharp minimum (the cavity mode) is observed (at 1370 and 680 nm for the first two orders). This minimum is the fingerprint of the microcavity, i.e. the PMA4 film sandwiched by the PVA films (see Figure 1b). Indeed, the cavity behaves as a structural defect both breaking the translation symmetry of the CA:PVK multilayer in the Bragg mirrors and acting as refractive index dopant (since its refractive index is different than that of CA and PVK). The overall effect is the formation of a cavity mode, whose spectral fingerprint is a sharp minimum within the reflectance peak associated with the PBG (in transmittance spectra the PBG reads as a minimum and the cavity mode as a maximum within it).[27] Indeed, photons resonant with the cavity modes are allowed to propagate through the structure thus reducing the reflectance of the sample or increasing its transmittance.[44,54] As predicted, the optical spectra of the microcavity also exhibit a second order PBG at about 680 nm (with cavity mode clearly observed) as well as a third order PBG whose spectral shape is less clear since it overlaps the absorption of PMA4 (about 450 nm). From the full width half maximum of the cavity mode at the first order PBG (about 37 nm), we estimate a cavity quality factor Q~40, in agreement with our previous findings with similar systems.[39,44,55]

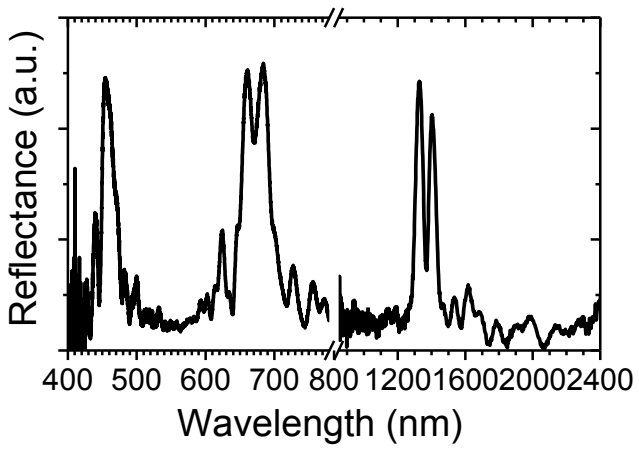

Fig. 5. Reflectance spectrum of the PMA4 microcavity.

We would like to stress that the spectral position of the cavity mode within the PBG is strongly dependent on the cavity optical path, i.e. the thickness times the refractive index of the cavity, while the PBG tuning is achieved during the growth by controlling DBR layers thicknesses and their dielectric contrast. When the photochromic transition is activated, the optical path of the cavity can be modified (changing Δn and perhaps the thickness of the defect layer) thus dephasing the light travelling through the cavity and allowing a fine spectral tuning of the cavity mode within the PBG.[26-27,30,44] For this reason, we studied the effect of CW optical writing/erasing on the microcavity's spectral response using a polarized source for writing. In Figure 6 we report the transmission spectra at the first order PBG after writing (in red) and after erasing (in blue) for the probing white light polarized like the writing beam (ULP, Figure 6a) and perpendicularly (unlike) to the writing beam (LP, Figure 6b). For ULP light polarization, the cavity mode is observed at 1322 nm after writing and at 1307 nm after erasing. This spectral shift (about 11 meV, 89 cm^{-1}) is fully reproducible and much larger than the spectral resolution of our spectrometer (8 cm^{-1}). On rotating the white light polarization to LP, the cavity mode is observed at 1318 and 1310 nm after writing and erasing processes, respectively. In this case the shift is 6 meV (48 cm^{-1}).

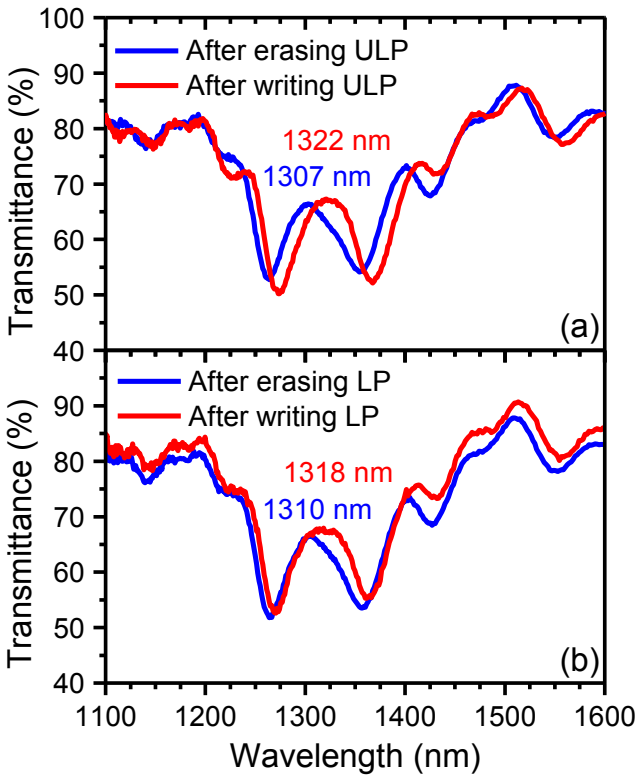

Fig. 6. Transmittance spectra of the microcavity first order PBG after irradiation with writing laser (red) and erasing laser (blue). The spectra were recorded with probing light polarized parallel/orthogonal to the one of the writing laser (ULP, panel a) / (LP, panel b).

It is worth to notice that the observed shift of the cavity is strongly anisotropic indicating that the isomerization process (even if not optimized) induces a significant in-plane chromophore orientation. This in turn induces a strong birefringence in the cavity affecting light propagation and finally photomodulating its optical response.

The very high quality of our microcavities is also evidenced by the observed photomodulation of the second order photonic band gap (as reported in Figure 7) indicating that these systems can be used to modulate at the same time multiple wavelengths. Figure 7a shows the transmission spectra for ULP probing light while the lower panel those for LP light polarization. Again, the defect mode's peak is visible and again a blue shift occurs after erasing just as was shown for the first order gap's cavity mode. The observed spectral shifts are 6 nm for the ULP and 3 nm for the LP, which correspond to 17 meV (~137 cm^{-1}) and 9 meV (~73 cm^{-1}), respectively. These shifts are much larger for both polarizations than those observed in the NIR for the first order cavity mode probably due to a pre-resonant enhancement effect of the PMA4 refractive index, which increases the optical path within the cavity. However, the ratio of the shifts (ULP/LP) observed for first and second order PBG is similar (about 1.9) indicating that the observed anisotropy is intrinsic and due to the same effect: the azo-chromophore orientation induced by the writing beam during the photoisomerization process. The erasing/writing shift of the cavity mode was successfully repeated for several irradiation cycles for both probing polarizations (see Figure SI1b of Supporting Information for the second order cavity mode). Moreover, for our irradiation conditions, the kinetics for the polarized writing process is faster than that for the

unpolarized erasing one (Figure SI1c of Supporting Information).

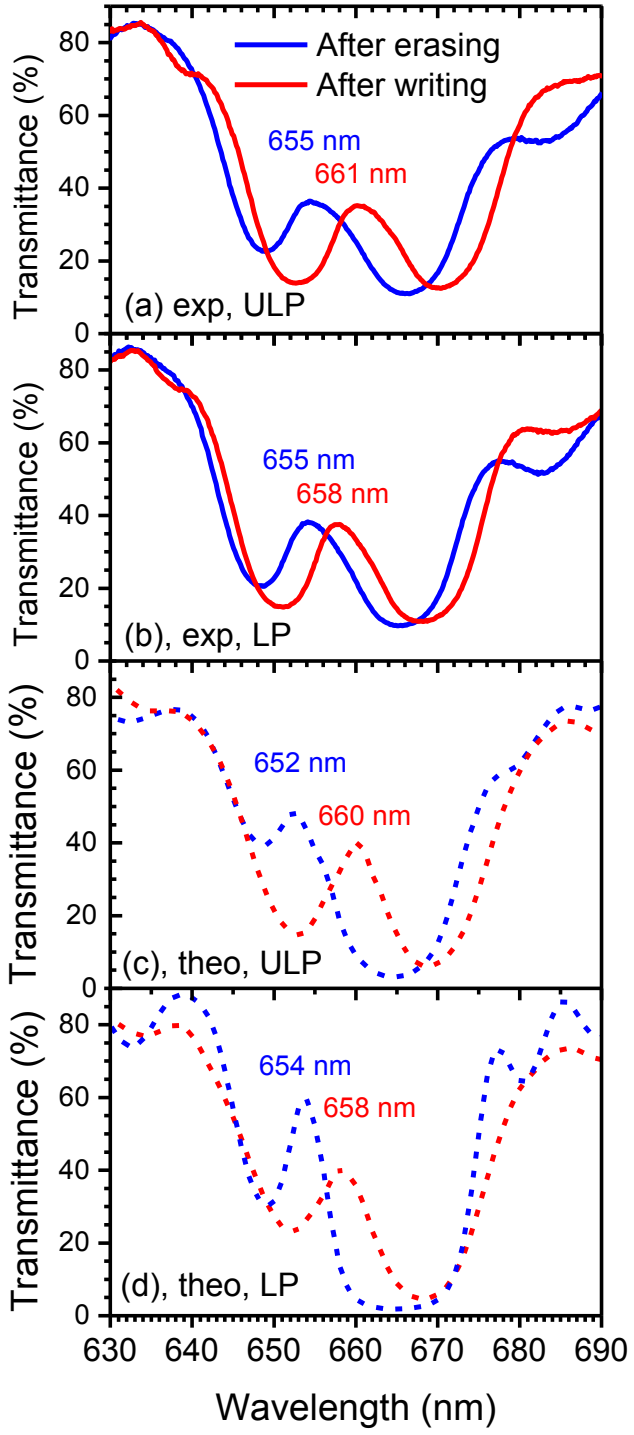

Fig. 7. Microcavity transmittance spectra at the second order PBG after irradiation with erasing laser (blue) and writing laser (red). The spectra have been recorded with light ULP (a) and LP (b) polarized light. Panel c and d show the calculated spectra (ULP and LP, respectively).

The larger shift induced by the writing beam on the second order photonic band gap also provides a very strong modulation of the transmitted light intensity. Indeed, at 655 nm a drop of transmittance by about 20% is observed. This value is comparable with the reflectivity change exploited for the DVD-RW technology[56].

Finally, minor modulation might be also expected for the third order photonic band gap. However, since such PBG overlaps the absorption of PMA4, the spectral details of the cavity mode are smeared out (see Figure SI4 in Supplementary Information). We would like to notice that in spite of the roughness induced by the isomerization process, the optical quality of our microcavities is surprisingly good and the photomodulation effects are spectrally and intensity well resolved. Moreover, the reversibility of the modulation after many writing/erasing cycles is clearly observed (see Fig. SI1b of Supporting Information).

Let's now focus on the dephasing effects induced by the all-optical photomodulation into the microcavity. The observed anisotropic shifts of the cavity mode can be interpreted as an effect of the change of the optical path within the cavity mode.[27,30] However, from the data reported in Figure 3d, no changes in film thickness are expected (within the experimental uncertainty) during photoisomerization, thus indicating that the observed changes are fully driven by Δn. The spectra were then simulated by using a home-made code based on the transfer matrix method, including the possible effect of disorder as detected by AFM and interference microscopy characterizations (upper limit of uncertainty in film thickness, ±5 nm for CA, PVK and PVA layers; ± 25 nm for PMA4 layer; roughness as in Fig 3).[57] The simulations reproduce very well the optical spectra (Figure 7c and 7d) and provide an estimate of the PMA4 refractive index. For the second order photonic band gap, we found for ULP polarization a refractive index of $n^w_{ULP} = 1.56$, $n^e_{ULP} = 1.47$ after writing and erasing, respectively (Figure 7c). For LP polarization, the modelling provides $n^w_{LP} = 1.50$, $n^e_{LP} = 1.46$ after writing and erasing, respectively (Figure 7d). Preliminary spectroscopic ellipsometry measurements were performed on PMA4 films, after writing. Comparison of data with simulations based on an isotropic, Kramers–Kronig consistent, multiple-resonance model, already successfully used on related systems,[58] allowed us to determine the complex index of refraction of the film in an extended spectral range (245–1700 nm). The value of n in the 630-690 nm, about 1.58-1.59, compares well, within experimental uncertainties, with the value suitable to fit the microcavity transmittance spectra as well as with recent literature data.[45] When the first order PBG spectral region is simulated, similar anisotropies are found with slightly reduced values of n as expected. The anisotropic change in refractive index between the two states achieved after writing and erasing is $\Delta n_{ULP} = 0.09$ ($^{\Delta n_{ULP}}/_{\bar{n}_{ULP}} = 6 \cdot 10^{-2}$) and $\Delta n_{LP} = 0.04$ ($^{\Delta n_{LP}}/_{\bar{n}_{LP}} = 3 \cdot 10^{-2}$), respectively ($\bar{n}$ is the average index after erasing and writing). These values are assigned to the joint effect of the isomerization process and to the concurrent birefringence induced by the mesogenic azo pendant chromophore in-plane oriented during the writing process. We notice that our normal incidence optical investigation does not allow to probe out-of-plane chromophore orientations, which has been recently reported [45]. We notice that a detailed analysis of the out-of-plane chromophore orientation when embedded within a microcavity is very complicate since affected not only by the azo-chromophore refractive index anisotropy, but also by the intrinsic anisotropy of the microcavity photonic band structure,[27] as well as by possible in-plane anisotropy of the thin PVA layers sandwiching the PMA4 film.[59] For all these reasons, the chromophore orientation can be investigated only

by incidence angle dependent spectroscopies joint to detailed optical modelling. Remembering that the photoisomerization process is not optimized since the writing wavelength is not fully resonant with the absorption at 300-350 nm, the results here reported are very stimulating and even stronger photomodulation effects can be envisaged for our all-polymer microcavities when resonant writing condition could be used.

In order to better highlight the quality of the photomodulation properties achieved by our microcavities, we compare them with data reported in literature for similar planar structures, i.e. distributed Bragg Reflectors and microcavities.[30,45] Yaghi et al. strongly modulated (by exploiting Δn) the dielectric contrast in a polymer DBR composed of 20 alternating PVA and liquid crystal azobenzene polyacrylate layers thus obtaining a deep change in the reflectance intensity at the PBG both by all-optical and mixed thermal/optical isomerization.[45] Noteworthy, they demonstrated that the azo-group shows spontaneous out-of-plane orientation when films of azo-functionalized polymers are prepared by spin-coating. The modulation they applied was unpolarized both at 365 nm (to randomly orient in-the-plane the azo groups) and at 346 nm (or by thermal annealing at the smectic phase, 80°C) to induce the out-of-plane orientation. We notice that in our case the photomodulation is substantially different since generating two phases possessing an in-plane random orientation of the chromophores (erasing, unpolarized 442 nm) and their partially in-plane oriented form (writing, polarized 405 nm). In spite of the reduced Δn exploited in our experiments and the much lower amount of photochromic material used (about 1 μm thick film instead of 20 layer of thickness 100-200 nm [45]), we have been able to achieved an excellent *anisotropic spectral modulation* of the microcavity modes for different diffraction orders. We also tried to modulate the optical response of our microcavities by thermal annealing but non-reversible spectral drifts have been observed (see Figure SI5 and SI6 of Supplementary Information).

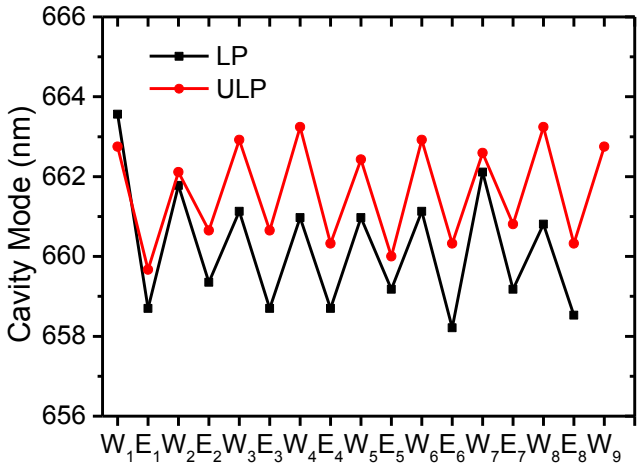

Fig. 8. Cavity mode photomodulation as a function of the writing/erasing cycles for LP (black) and ULP (red) probing polarization.

Finally, we checked the repeatability of all-optical CW modulation for our microcavities, as required for photonic applications for both LP and ULP probing polarization (Fig. 8). A good reversibility upon several cycles of writing/erasing processes is observed. Notice that the reversibility is fine independently on possible generation of roughness in the cavity layer upon irradiation (see Fig. 3). The reversibility observed for our microcavities is in full agreement with previously reported data for DBRs.[45]

A more direct comparison with our data can be done with microcavities made by inorganic mirrors, which are widely used in photonics. Piron et al. prepared a 639 nm thick microcavity containing a polymethyl methacrylate carrying a Disperse Red One pendant group sandwiched between two zirconia:silica DBR mirrors.[30] In spite of the larger dielectric contrast of such DBRs (~0.6) with respect to our all-polymer system (~0.2), which allows for a stronger light confinement within the microcavity,[27] they recorded under picosecond pulsed modulation a shift of the cavity mode by about 3.5 nm at 1380 nm. This value is much lower than those here reported for a just slightly thicker cavity, where simultaneous photomodulation of cavity modes for different order photonic band gaps (i.e. different wavelengths) can be achieved.

A final remark on the interest for all-polymer planar PhCs is related to their mechanical properties allowing to peel-off such structures from the substrate where they were grown, thus being suitable for post-growth implementation into optical devices and circuitries (even on curved surfaces), with obvious advantages with respect to the correspondent inorganic systems.

In view of all such results, the CW all-optical spectral modulation here reported are remarkable. Even larger effects can be envisaged when the writing procedure could be optimized and pulsed excitation used. Moreover, the film roughness induced in PMA4 film by the writing/erasing process does not significantly affect the switching process and its reversibility. Our results, joined to the simple preparation technique as well as to the possibility to have free-standing films, represent a proof-of-concept for the development of all-polymer photomodulators working in different spectral ranges.

Conclusions

We have prepared high optical quality all-polymer planar microcavities containing a photochromic azobenzene polymethacrylate. A reversible all-optical photomodulation of the spectral response is achieved by back-and-forth photoisomerization through polarized 405 nm and unpolarized 442 nm CW lasers. In spite of a non-optimized writing procedure as well of the increased roughness upon photoexcitation, the photochromic transition induces a remarkable and anisotropic reversible change of the spectral properties of the cavity modes for different diffraction orders both in the NIR and VIS spectral ranges associated with a strong change in transmittance. The photomodulation properties have been accounted for by a suitable optical model considering the disorder in the structure as well as the surface corrugations modulated on spatial domain larger than 500 nm induced by illumination. These all-polymer microcavities, which can be removed from the substrate as free-standing films and applied to any surface, can be

considered for the development of innovative applications to laser switches, limiters and modulators.

Acknowledgements

This work was supported by the Italian Ministry of the University and Scientific and Technological Research trough the project 2010XLLNM3 (PRIN 2010-2011).

References

[1] T. Ikeda, J.-i. Mamiya, Y. Yu, *Angew. Chem. Int. Ed.* 2007; 46: 506-528.
[2] Y. Kuwahara, M. Kaji, J. Okada, S. Kim, T. Ogata, S. Kurihara, *Mater. Lett.* 2013; 113: 202-205.
[3] M. McCullagh, I. Franco, M. A. Ratner, G. C. Schatz, *J. Am. Chem. Soc.* 2011; 133: 3452-3459.
[4] A. A. Beharry, G. A. Woolley, *Chem. Soc. Rev.* 2011; 40: 4422-4437.
[5] S. W. Basuki, V. Schneider, T. Strunskus, M. Elbahri, F. Faupel, *ACS Appl. Mater. Interfaces* 2015; 7: 11257-11262.
[6] V. Schneider, T. Strunskus, M. Elbahri, F. Faupel, *Carbon* 2015; 90: 94-101.
[7] M. Scalora, J. P. Dowling, C. M. Bowden, M. J. Blomer, *Phys. Rev. Lett.* 1994; 73: 1368.
[8] H. M. D. Bandara, S. C. Burdette, *Chem. Soc. Rev.* 2012; 41: 1809-1825.
[9] G. Bergamini, P. Ceroni, A. Credi, M. Venturi, K. Yager, V. Balzani, D. A. Leigh, A. Yousefi-Koma, Q. M. Zhang, M. Zrinyi, L. McDonald Schetky, F. Gordaninejad, R. Kornbluh, F. T. Mak Arthur, Y. Osada, M. Behi, M. Shahinpoor, *Intelligent Materials*. The Royal Society of Chemistry: 2008.
[10] O. Tsutsumi, T. Shiono, T. Ikeda, G. Galli, *J. Phys. Chem. B* 1997; 101: 1332-1337.
[11] M. Yamamoto, K. Kinashi, Y. Koshiba, Y. Ueda, N. Yoshimoto, *Thin Solid Films* 2008; 516: 2686-2690.
[12] M. Han, D. Ishikawa, T. Honda, E. Ito, M. Hara, *Chem. Commun.* 2010; 46: 3598-3600.
[13] Y. Koshiba, M. Yamamoto, K. Kinashi, M. Misaki, K. Ishida, Y. Oguchi, Y. Ueda, *Thin Solid Films* 2009; 518: 805-809.
[14] M. Moritsugu, S.-n. Kim, S. Kubo, T. Ogata, T. Nonaka, O. Sato, S. Kurihara, *React. Funct. Polym.* 2011; 71: 30-35.
[15] A. A. Beharry, O. Sadovski, G. A. Woolley, *J. Am. Chem. Soc.* 2011; 133: 19684-19687.
[16] S. Atsushi, T. Osamu, K. Akihiko, S. Takeshi, I. Tomiki, T. Naoto, *J. Am. Chem. Soc.* 1997; 119: 7791-7796.
[17] H. Kurihara, A. Shishido, T. Ikeda, *J. Appl. Phys.* 2005; 98: 083510.
[18] M. Kamenjicki, I. K. Lednev, S. A. Asher, *J. Phys. Chem. B* 2004; 108: 12637-12639.
[19] A. Natansohn, P. Rochon, *Chem. Rev.* 2002; 102: 4139-4175.
[20] A. Priimagi, M. Kaivola, F. J. Rodriguez, M. Kauranen, *Appl. Phys. Lett.* 2007; 90: 121103.
[21] A. Stracke, J. H. Wendorff, J. Mahler, G. Rafler, *Macromolecules* 2000; 33: 2605-2609.
[22] K. Okano, A. Shishido, T. Ikeda, *Macromolecules* 2006; 39: 145-152.
[23] S. Menghetti, M. Alderighi, G. Galli, F. Tantussi, M. Morandini, F. Fuso, M. Allegrini, *J. Mater. Chem.* 2012; 22: 14510-14517.
[24] F. Tantussi, S. Menghetti, E. Caldi, F. Fuso, M. Allegrini, G. Galli, *Appl. Phys. Lett.* 2012; 100: 083103.
[25] R. M. Parker, J. C. Gates, H. L. Rogers, P. G. R. Smith, M. C. Grossel, *J. Mater. Chem.* 2010; 20: 9118-9125.
[26] J. D. Joannopulos, R. D. Meade, J. N. Win, *Photonic Crystals: Molding the Flow of the Light* Princeton University Press: Princeton, 1995.
[27] D. Comoretto, *Organic and Hybrid Photonic Crystals*. 1 ed.; Springer International Publishing: 2015; p XXI, pp 497.
[28] M. D. Tocci, M. Scalora, M. J. Bloemer, J. P. Dowling, C. M. Browden, *Phys. Rev. A* 1996; 53: 2799.
[29] J. C. Hong, J. H. Park, C. Chun, D. Y. Kim, *Adv. Funct. Mater.* 2007; 17: 2462-2469.
[30] R. Piron, E. Toussaere, D. Josse, J. Zyss, *Appl. Phys. Lett.* 2000; 77: 2461-2463.
[31] Y. Huang, W. Liang, J. K. S. Poon, Y. Xu, R. K. Lee, A. Yariv, *Appl. Phys. Lett.* 2006; 88: 181102.
[32] F. Gallego-Gómez, A. Blanco, D. Golmayo, C. López, *Adv. Funct. Mater.* 2011; 21: 4109-4119.
[33] H. Coles, S. Morris, *Nat Photon* 2010; 4: 676-685.
[34] C. Fenzl, T. Hirsch, O. S. Wolfbeis, *Angew. Chem. Int. Ed.* 2014; 53: 3318-3335.
[35] M. Kamenjicki Maurer, I. K. Lednev, S. A. Asher, *Adv. Funct. Mater.* 2005; 15: 1401-1406.
[36] S. Li, M. Fu, Y. Zhang, J. Duan, D. He, Y. Wang, *J. Mater. Chem. C* 2013; 1: 5072-5077.
[37] Z. Z. Gu, T. Iyoda, A. Fujishima, O. Sato, *Adv. Mater.* 2001; 13: 1295-1298.
[38] P. Lova, G. Manfredi, L. Boarino, A. Comite, M. Laus, M. Patrini, F. Marabelli, C. Soci, D. Comoretto, *ACS Photonics* 2015; 2: 537-543.
[39] L. Frezza, M. Patrini, M. Liscidini, D. Comoretto, *J. Phys. Chem. C* 2011; 115: 19939-19946.
[40] L. Fornasari, F. Floris, M. Patrini, G. Canazza, G. Guizzetti, D. Comoretto, F. Marabelli, *Appl. Phys. Lett.* 2014; 105: 5.
[41] V. M. Menon, M. Luberto, N. V. Valappil, S. Chatterjee, *Opt. Express* 2008; 16: 19535-19540.
[42] N. V. Valappil, M. Luberto, V. M. Menon, I. Zeylikovich, T. K. Gayen, J. Franco, B. B. Das, R. R. Alfano, *Photonic Nanostruct.* 2007; 5: 184-188.
[43] L. M. Goldenberg, V. Lisinetskii, S. Schrader, *Appl. Phys. B* 2015: 1-7.
[44] G. Canazza, F. Scotognella, G. Lanzani, S. D. Silvestri, M. Zavelani-Rossi, D. Comoretto, *Laser Phys. Lett.* 2014; 11: 035804.
[45] R. Yagi, H. Katae, Y. Kuwahara, S.-N. Kim, T. Ogata, S. Kurihara, *Polymer* 2014; 55: 1120-1127.
[46] M. Moritsugu, T. Ishikawa, T. Kawata, T. Ogata, Y. Kuwahara, S. Kurihara, *Macromol. Rapid Commun.* 2011; 32: 1546-1550.
[47] A. L. Álvarez, J. Tito, M. B. Vaello, P. Velásquez, R. Mallavia, M. M. Sánchez-López, S. Fernández de Ávila, *Thin Solid Films* 2003; 433: 277-280.
[48] F. Scotognella, S. Varo, L. Criante, S. Gazzo, G. Manfredi, R. Knarr, D. Comoretto, Spin-Coated Polymer and Hybrid Multilayers and Microcavities In *Organic and Hybrid Photonic Crystals*, Comoretto, D., Ed. Springer: 2015; 77-101.
[49] T. Komikado, A. Inoue, K. Masuda, T. Ando, S. Umegaki, *Thin Solid Films* 2007; 515: 3887–3892.
[50] I. Horcas, R. Fernández, J. M. Gómez-Rodríguez, J. Colchero, J. Gómez-Herrero, A. M. Baro, *Rev. Sci. Instrum.* 2007; 78: 013705.
[51] A. S. Angeloni, D. Caretti, C. Carlini, E. Chiellini, G. Galli, A. Altomare, R. Solaro, M. Laus, *Liq. Cryst.* 2006; 33: 1302-1311.
[52] K. E. Snell, N. Stéphant, R. B. Pansu, J.-F. Audibert, F. Lagugné-Labarthet, E. Ishow, *Langmuir* 2014; 30: 2926-2935.
[53] We notice that with interference microscopy, no significant changes in thickness is observed between the different films thus suggesting a possible uncertainty with this technique larger than 3%.

[54] S. Gazzo, G. Manfredi, R. Poetzsch, Q. Wei, M. Alloisio, B. Voit, D. Comoretto, *J. Polym. Sci. B: Polym. Phys.* 2015, DOI:10.1002/polb.23932.
[55] The quality factor Q achieved in inorganic semiconductors when photonic structures are created by photo- or electron-lithography can be orders of magnitude larger than that obtained with spin-coated microcavities. The former are extremely precise but at high money, time and energy costs. Just to provide the reader with some figures for our multilayered structures, the interlayer roughness of our DBR structures is of the order of 1 nm for a layer thickness of more than 100 nm. While such a 1% roughness is suitable for the scope of this work, it is not comparable with that achieved in inorganic materials where the roughness could be comparable to few atomic layers. This roughness dramatically affects the quality factor of the spin-coated microcavities. An additional factor affecting Q is the thickness control over the large area of our systems (about 1 squared inch). In this case, polymer processability plays a major role, in particular when thick films, as those needed for photomodulation, are used. For very highly processable polymers, larger values of Q have been achieved for reduced cavity thicknesses than those here used. Indeed, for thinner PMA4 microcavities (about 600 nm), the cavity factor observed rises to about 80, in full agreement with our previous findings for fluorescent spin-cast microcavities [39, 44, 48].
[56] G.-F. Zhou, *Mat. Sci. Eng. A* 2001; 304–306: 73-80.
[57] M. Skorobogatiy, J. Yang, *Fundamentals of Photonic Crystal Guiding* Cambridge University Press: 2009.
[58] C. Toccafondi, L. Occhi, O. Cavalleri, A. Penco, R. Castagna, A. Bianco, C. Bertarelli, D. Comoretto, M. Canepa, *J. Mater. Chem. C* 2014; 2: 4692-4698.
[59] M. Campoy-Quiles, P. G. Etchegoin, D. D. C. Bradley, *Phys. Rev. B* 2005; 72: 045209.

Author Contributions

The manuscript was written through contributions of all authors. All authors have given approval to the final version of the manuscript.
R.J. Knar III prepared the microcavities and made the optical characterizations. G. Manfredi made the simulations of the optical response for both microcavities and DBR. E. Martinelli, M. Pannocchia, and G. Galli synthesized PMA4, characterized its properties and separated their high molecular weight fractions. G. Galli also coordinated the synthetic strategies. D. Repetto, C. Mennucci, and F. Buatier de Mongeot investigated the morphology of the films and their thicknesses. I. Solano and M. Canepa did the ellipsometric measurements. D. Comoretto conceived and managed the overall project as well as the PhC preparation and characterization.